Министерство науки и высшего образования Российской Федерации

Администрация Правительства Кузбасса

Научно-образовательный центр мирового уровня «Кузбасс»

Сибирский государственный индустриальный университет

Посвящается 100-летию
со дня рождения ректора СМИ,
доктора технических наук,
профессора Н.В.Толстогузова

МЕТАЛЛУРГИЯ: ТЕХНОЛОГИИ, ИННОВАЦИИ, КАЧЕСТВО

«Металлургия – 2021»

Труды
XXII Международной научно-практической конференции

10 – 11ноября 2021 г.

Часть 1

Новокузнецк
2021

ISSN 2542-1670

УДК 669(06)+658.012.056(06)
М 540

М 540 Металлургия : технологии, инновации, качество : труды XXII Международной научно-практической конференции. В 2 частях. Часть 1 / под общ. ред. А.Б. Юрьева, Сиб. гос. индустр. ун-т. – Новокузнецк : Изд. центр СибГИУ, 2021. – 326 с. : ил.

Труды конференции включают доклады по актуальным вопросам теории и наукоемким технологиям металлургических процессов, обработки металлических материалов: литейное производство, обработка давлением, термическая обработка.

ОРГАНИЗАТОРЫ И ПАРТНЕРЫ КОНФЕРЕНЦИИ

Администрация Правительства Кузбасса
ФГБОУ ВО «Сибирский государственный индустриальный университет»
АО «ЕВРАЗ ЗСМК»
АО «Русал-Новокузнецк»
АО «Кузнецкие ферросплавы»
АО «НЗРМК им. Н.Е. Крюкова»
Ляонинский университет науки и технологии, г. Аньшань, КНР
ОАО «Черметинформация»
Издательство Сибирского отделения РАН
Журнал «Известия вузов. Черная металлургия»
Журнал «Вестник СибГИУ»
Журнал «MATEC Web of Conferences »
Научно-образовательный центр мирового уровня «Кузбасс»
АО «Кузбасский технопарк»
Западно – Сибирское отделение Российской Академии естественных наук
Совет молодых ученых Кузбасса

УДК 539.098

ВЛИЯНИЕ МАГНИТНОГО ПОЛЯ НА МИКРОСТРУКТУРУ, МИКРОТВЕРДОСТЬ И КОРРОЗИОННЫЕ СВОЙСТВА СТАЛИ 9CRMOV-N ИЗГОТОВЛЕННОЙ МЕТОДОМ ПРОВОЛОЧНО-ДУГОВОГО АДДИТИВНОГО ПРОИЗВОДСТВА

Осинцев К.А.[1,2], Шляров В.В. [1,3], Чэнь С.[1,2], Коновалов С.В.[1,2], Загуляев Д.В.[1,3], Чаплыгин К.К.[2]

[1]Университет Вэньчжоу, Вэньчжоу, Китай, ksv@ssau.ru
[2]Самарский национальный исследовательский университет им. академика С.П. Королева, Самара, Россия
[3]Сибирский государственный индустриальный университет, Новокузнецк, Россия

Аннотация. *При изготовлении материала в несколько слоев мы применяли магнитное поле (величина индукции 0,2 Тл) для ускорения повторного перемешивания частиц материала в сварочной ванне, тем самым уменьшая количество потенциальных дефектов в структуре. Образцы, полученные как в магнитном поле, так и вне его, обладали ферритно-мартенситной структурой. Исследование установило уменьшение количества пор на 6,12 % и сокращение на 41,81 % из-за применения магнитного поля при наплавке.*

Ключевые слова: *Проволочно-дуговое аддитивное производство, хромистая сталь, коррозия, магнитное поле, жаропрочность, пористость, микротвердость.*

THE EFFECT OF MAGNETIC FIELD ON MICROSTRUCTURE, MICROHARDNESS AND CORROSION PROPERTIES OF WIRE-ARC ADDITIVE MANUFACTURED STEEL 9CRMOV-N

Osintsev K.A.[1,2], Shlyarov V.V.[1,3], Chen S.[1,2], Konovalov S.V.[1,2], Zaguliaev D.V.[1,3], Chaplygin K.K.[2]

[1]Institute of Laser and Optoelectronic Intelligent Manufacturing, Wenzhou University, Wenzhou, P. R. China, ksv@ssau.ru
[2]Samara National Research University, Samara, Russia
[3]Siberian State Industrial University, Novokuznetsk, Russia

Abstract. *When manufacturing the material in multiple layers, we applied a magnetic field (a value of induction 0.2 T) to accelerate the remixing of material particles in a weld pool, thus reducing the number of potential defects in the structure. Samples obtained both in and out of a magnetic field possessed a ferrite-martensite structure. The research has established a 6.12 % decrease in a number of pores and 41.81 % shrinking due to a magnetic field's application when surfacing.*

Key words. *Wire arc additive manufacturing, chromium steel, corrosion, magnetic field, heat resistant, porosity, microhardness.*

1. Introduction

The increasing operating temperature and pressure of thermal power stations may exert a beneficial effect on their efficiency factor, reducing, therefore, an amount of carbon dioxide emission. Any improvement in the efficiency factor may be useful for the environment. A fundamental problem related to the increased operating temperature and pressure of electric power plants is synthesizing a material capable of the work at high temperatures. A group of steels 9Cr-1Mo represents most prospective materials for such high-temperature applications. These alloys possess sufficient high-temperature stability and corrosion resistance, unlike low-chromium ferrite heat resistant steels and replace more frequently austenitic stainless steels ultra-supercritical thermal stations [1]. Advanced anti-corrosion properties and low creep rates are possible due to a significant percentage of chromium and hard-melting transition metals, such as W, Mo, V, Nb, and Ta [2]. Compared to austenitic stainless steels, ferrite-martensite steels are better resistant to the neutron-induced swelling, and its creep rate is lower if irradiated. Thus, they can be used in the nuclear power industry as an engineering material [3].

Wire arc additive manufacturing is supposed to be one of the future production processes to output articles from heatproof materials. Additive technologies provide a substantial reduction in economic and material resources required to manufacture tooling in traditional manufacturing, lower an amount of necessary material, and waste, making it more environmentally friendly. The output of thermal power engineering products is maximally efficient, provided that wire arc additive manufacturing technologies are applied for a high deposition rate, reasonable costs of raw materials (wire), and a possibility to produce space-consuming objects. To illustrate, researchers [4,5] have shown a prospect of fabricating large-sized goods from alloy 9CrMoV-N with high impact ductility and microhardness. By the way, wire arc additive manufacturing suffers from certain drawbacks like the pore formation and various defects, e.g., dislocations and martensite-austenitic fragments [5].

Since wire arc additive manufacturing is similar to multi-path fusion welding, we may use methods accepted in welding and surfacing to control a defect formation process. One of such techniques is the application of transversal and linear magnetic fields [6,7] when melting a metal. To be more precise, in arc welding and wire surfacing, a linear or transversal magnetic field increases the melting factor of an electrode metal, provides control over the penetration depth of base metal, and furthers grains' refinement adapts strength characteristics. To sum up, applying a magnetic field in wire arc additive manufacturing may slow down the defect formation and improve output heatproof materials' properties. Hence, this study aims to explore a magnetic field influence on the structure and properties of wire arc additive manufactured steel 9CrMoV-N.

2. Materials and methods

In our experiments we used 9CrMoV-N steel wire with a diameter of 1.2 mm, the microhardness of 265 HV and the following chemical composition, is presented in table 1.

Table 1 - Chemical composition of 9CrMoV-N steel wire, (wt. %)

C	Mn	Si	S	P	Cr	Ni	Mo	Nb	V	N	Cu	Al
0.08-0.13 %	0.40-0.80 %	0.15-0.50 %	≤ 0.010 %	≤ 0.010 %	8.5-9.5 %	0.40-0.80 %	0.85-1.10 %	0.03 %	0.15-0.25 %	0.03-0.07 %	≤ 0.10 %	≤ 0.40 %

For the wire arc additive manufacturing of steel 9CrMoV-N samples, we adapted the cold metal transfer technology and used a welding machine Fronius CMT Advanced 4000R, and a numerically controlled 6-Axis Robot FANUC Robot M-10iA intended for the multifunctional wire feed in argon-arc welding (Institute of Laser and Optoelectronics Intelligent Manufacturing, Wenzhou University, China). Layer deposition parameters were set using a controller RCU 5000i to adjust a nozzle motion velocity along the base surface, a wire feed speed, as well as values of current and voltage. In our experiments, the parameters were as follows: the deposited layer thickness – 6 mm, the wire feed speed – 6 m/minute, the amperage I = 195 A, the voltage U = 15.5 V. When layering, a welding nozzle was oriented perpendicular to the base surface. We took a 300 mm long 200 mm wide and 15 mm high carbon steel Q345 plate as a base. Before the layers' deposition, a plate surface was machined with a grinder; impurities and oxides were removed with acetone. A mixture (80% Ar and 20% CO_2) was used as a shielding gas consumed at 20 l/min.

For the additive manufacturing of samples in a constant magnetic field, we set parameters identically to layering without a magnetic field. To create a magnetic field, we used an electromagnet WD-175 and a programmable direct current source RA-3KW (the voltage and current were U = 4.6 B and I = 0.73 A, respectively). The magnetic field induction was perpendicular to the direction of the layer deposition. To measure the induction of a magnetic field, a high-precision digital gaussmeter CH-1500 was applied; its value was 0.2 T.

For metallographic studies, samples were cut from the center of fabricated semi-finished products by an electro-erosion cutting machine, finished them using abrasive paper with various grain fineness numbers, and polished them with a chromium oxide paste. Then they were etched in the solution containing 47.5% HCl, 47.5% H_2O, and 5% HNO_3. Etching time was 20 minutes. Microstructure analysis was carried out by an optical microscope METAM PB-34.

The porosity was examined by a scanning laser microscope Olympus LEXT OLS4100, which combines a motorized optical microscope for research purposes and a laser scanning microscope.

X-ray photographs were taken by an X-ray diffractometer DRON-7 (Innovation Center Bourevestnik, Russia) in the following conditions: emission CuKα, wavelength, λ=1.5418 Å, cathode voltage, U = 40 kV, current, I = 20 mA, shooting interval 11-100º, scanning pitch, hθ = 0.1º, scanning time in a point, τ = 10 s. To filter β-emission, a nickel filter was used.

The microhardness of obtained samples was measured in the cross-section with an interval of 5 mm by the Vickers method. The indenter was loaded 1.96 N (a hardness testing machine HXD–1000TM/LCD), a period of load applying and keeping – 15 s, an unloading period – 5 s. A minimum of five measurements was carried out at each point.

Since the ferrite-martensite steel 9CrMoV-N is corrosion resistant and machine elements manufactured from it may be used in nuclear and thermal engineering, corrosion tests of obtained samples were conducted as specified in ASTM G31-72 (2004). The method involves determining a metal weight loss per a surface unit of samples when kept in aggressive conditions. A test medium is a model CO_2-containing solution: 17 g/l NaCl, 2 g/l CaCl2, and 0.2 g/l $MgCl_2$. The solution is enriched with CO_2 at a pressure of 1 atm. to full saturation. A test temperature was set at 20 °C.

Before performing tests on samples, they were labeled and washed properly in acetone. Defatted samples were dried up in a hot air current (in a temperature range from 40 to 50 °C) for 10-15 minutes. Figure 1 presents samples prepared for corrosion testing.

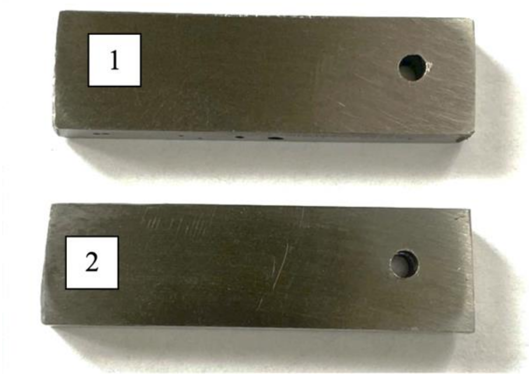

Figure 1 - Steel 9CrMoV samples prepared to corrosion stability tests
(1 – produced without a magnetic field, 2 – in a magnetic field)

Then cleaned samples were positioned vertically in a cell holder. Here, samples were separated from a holder, each other, and cell walls; a free contact with a corrosion medium was provided. The duration of the tests was 100 hours.

To determine a corrosion rate of test samples we used the formula:

$$\rho = \frac{m_1 - m_2}{s \cdot \tau}, \text{ g/m}^2\text{h}, \tag{1}$$

where ρ – corrosion rate, g/m^{2}h, m_1 – sample weight before testing, g, m_2 – sample weight after testing, g, s – sample surface area, m^2, test period, h.

A corrosion rate determined in g/m^{2}h was recalculated in mm per year according to the following formula:

Corrosion rate

$$= (g/m\text{^}2 \cdot h \cdot 8760)/(sp.weight \cdot 1000) = g/m\text{^}2 \cdot h \cdot \text{К} = mm/year, \tag{2}$$

where К – a recalculation coefficient for the corrosion rate, which is as high as 1.14 for a chromium steel.

3. Research results and discussion

3.1 Metallography

In the process of wire arc additive manufacturing based on the cold metal transfer technology, we fabricated 60×6×100 mm parallelepiped steel 9CrMoV-N samples containing 30 layers of the deposited metal (Figure 2).

Figure 2 - Wire arc additive manufactured steel 9CrMoV-N samples
(a – produced without a magnetic field, b – in a magnetic field (side view))

A sample of steel 9CrMoV-N fabricated by the cold metal transfer method in the field of a constant magnet possesses a ferrite-martensite structure similar to a sample not affected by a magnetic field when manufactured. Figure 3 visualizes the microstructure of the steel. The examination of micro-sections has pointed out that the lath martensite forms the microstructure of obtained samples with various lath directions. The ferrite is shown as white regions in the microphotograph; martensite laths are black-colored.

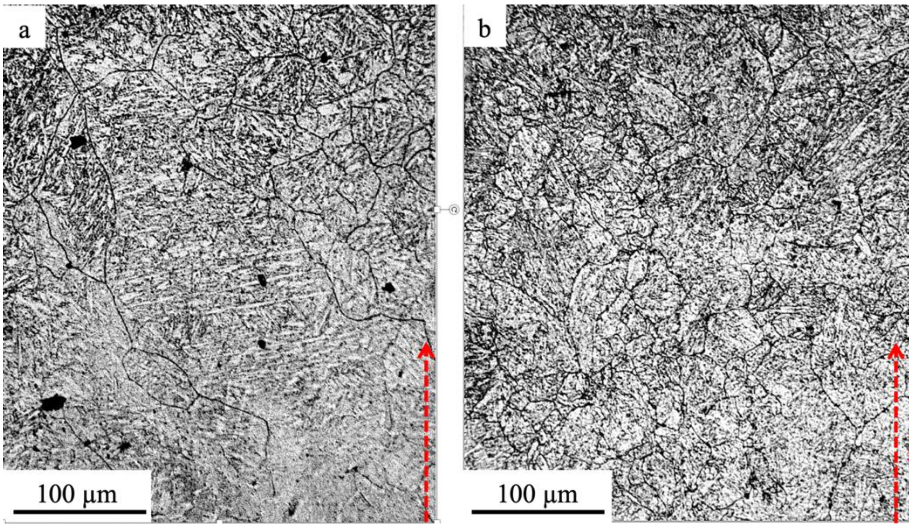

Figure 3 - The microstructure of wire arc additive manufactured steel 9CrMoV-N
(a – produced without a magnetic field applied; b – in a magnetic field). Dashed arrows indicate the direction of sample composition.

Grains of steel untreated by a magnetic field when produced are in a range 36 ± 2 µm with the error probability of 5 %, the Student's coefficient around 1.97, and the relative error of 6 % (Figure 3, a). The grain size in a sample formed in a magnetic field is 23 ± 1 µm with the error probability of 5 %, the Student's coefficient around 1.97, and the relative error of 5% (Figure 3, b). The data obtained suggest the effect of a magnetic field in the wire arc additive manufacturing of steel 9CrMoV-N results in the almost 1.5 times refinement of grains.

The study on the porosity of samples with a scanning laser microscope has found numerous spherical pores in their microstructure (Figure 4).

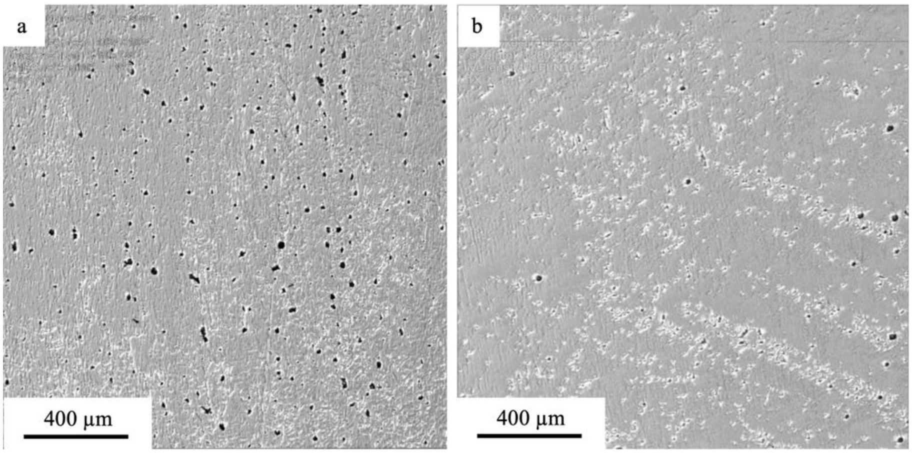

Figure 4 - The analysis of pores in low-alloyed wire arc additive manufactured steel 9CrMoV-N (a – produced without a magnetic field applied; b – in a magnetic field).

In general, we suggest two reasons for the pore formation: the poor quality of input raw materials and the specifics of the wire arc additive manufacturing technology [8]. Pores with a form like spheres develop from gases, which fail to surface due to the rapid crystallization of a deposited layer, whereas irregular pores result from an inappropriate layering mode and not completely dissolved particles of the material [9]. The microstructure examination has revealed only spherical pores in samples of interest; irregular pores were undetected. Therefore, we suggest pores formed in examined samples owing to the gas generation induced by chemical reactions. First, CO is a product of the reaction between oxygen and carbon in the molten pool:

$$[C] + [O] = CO \tag{4}$$

Secondly, the metal's surface layer gets oxidized, and oxide impurities can be transported into the melt pool [10]. Then a metal oxide can react with the carbon dissolved in a weld pool. Therefore, a more considerable amount of carbon dioxide emits in the molten metal:

$$[C] + [FeO] = Fe + CO \tag{5}$$

$$[C] + [MnO] = Mn + CO \tag{6}$$

$$2[C] + [SiO_2] = Si + 2CO \tag{7}$$

Finally, a shielding gas may be transported into the melt pool when layering.

Our studies have revealed 0.676 pores per 1 µm^2 on average in the wire arc additive manufactured steel without applying a magnetic field; their average size is 25.028 µm. If the surfacing is affected by a magnetic field, 0.637 pores on average are detected per 1 µm^2 of the material; their size is 14.564 µm. To summarize, a magnetic field's influence when layering results in a 6.12% decrease of the pores quantity and a 41.81% reduction in their size. A perpendicular magnetic field accelerates the release of gases formed in the weld pool due to the Lorentz force affecting the molten metal [10].

3.2 X-ray diffraction analysis

The steel 9CrMoV-N can contain any of the following phases: carbides or carbonitrides $M_{23}C$, M(C, N), M_2 (C, N), M_7C_3, $M_{23}C_6$ (M designates any element of a host metal Fe, Cr, Mn, V, Nb, Mo) and other phases. The process of phase transformations in steels 9CrMoV-N is generalized as follows:

$$M_3C + MC \rightarrow M_3C + MC + M_{23}C_6 \rightarrow M_3C + MC + M_{23}C_6 + M_7C_3 \rightarrow\rightarrow MC + M_{23}C_6 + M_7C_3 \tag{8}$$

Figure 5 presents X-ray diffraction patterns of samples obtained via wire arc additive manufacturing in and out of a magnetic field. A sample not affected by a magnetic field when fabricated an X-ray phase analysis detected phases containing Mn and Cr with a chemical structure $Mn_{23}C_6$,

Mn_7C_3, NbN, VN, Fe_7W_6, Fe_7C_3, Fe_3C, Cr_7C_3 and Cr_2N. In a sample exposed to a magnetic field, the same phases are identified but with a higher peak intensity.

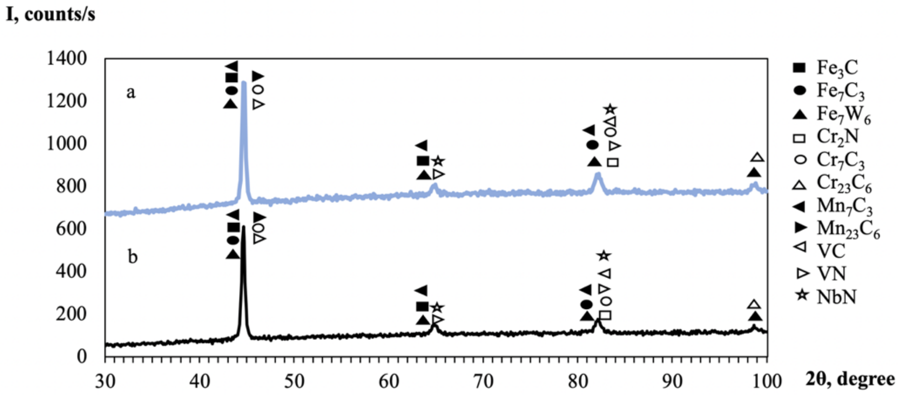

Figure 5 - X-ray diffraction patterns of samples in and out of a magnetic field
(a – produced without a magnetic field applied; b – in a magnetic field).

3.3 Microhardness test results

Figure 6 illustrates the results of the microhardness testing. A sample's microhardness unaffected by a magnetic field when fabricated ranges from 358 to 454 HV, whereas this characteristic varies from 553 to 651 HV for a sample produced in a magnetic field. Such a value range ~100 HV depends on the specifics of the wire arc additive manufacturing process, when each layer is exposed to diverse thermal cycles, resulting in the heterogeneity of properties in different layers. A mean value of the microhardness in a sample not exposed to a magnetic field is determined to be 406 ± 6 HV; that is 1.52 times higher than the input wire (this value is given in 2.1). The application of a magnetic field when wire arc additive manufacturing raised a mean value of the microhardness to 591 ± 7 HV; that as almost twice as higher as the microhardness of the input wire; the hardness of a sample unaffected by a magnetic field was 1.46 times higher. We suggest the improved microhardness of samples produced in a magnetic field results from the grain refinement, which causes the grain-boundary strengthening according to the Hall-Petch relationship:

$$HV = H_0 + k_H d^{-\frac{1}{2}}, \tag{9}$$

where HV – measured microhardness of a material;

H_0 – microhardness of a material mono-crystal;

k_H – a material characterizing coefficient, it equals to the slope of curves in the function graph HV on $D^{-1/2}$;

d – grain size.

The investigation on micro-sections has highlighted a mean grain size is almost 1.5 times smaller. Assuming the stability of coefficients H_0 and k_H, we obtain:

$$\frac{HV_{mf}}{HV_{nmf}} = \sqrt{\frac{d_{nmf}}{d_{mf}}} = \sqrt{1.5} = 1.22, \tag{10}$$

where HV_{mf} – the determined microhardness of a sample produced in a magnetic field;

HV_{nmf} – the determined microhardness of a sample unexposed to a magnetic field;

d_{nmf} – a mean grain size in a sample unaffected by a magnetic field;

d_{mf} – a mean grain size in a sample exposed to a magnetic field.

There is a 16 % difference between a resultant microhardness ratio of samples affected and unaffected by a magnetic field determined according to (10) and measured experimentally. Because of assumptions, an experimentally obtained a 1.5 increase in the mean microhardness complies with the Hall-Petch relation.

To be more precise, we address the graph presented in Figure 6. The maximal value of the microhardness is observed 70 mm beneath the base. This phenomenon is attributed to the accumulation of less heat in upper layers of a sample resulting in grain refinement and a microhardness increase.

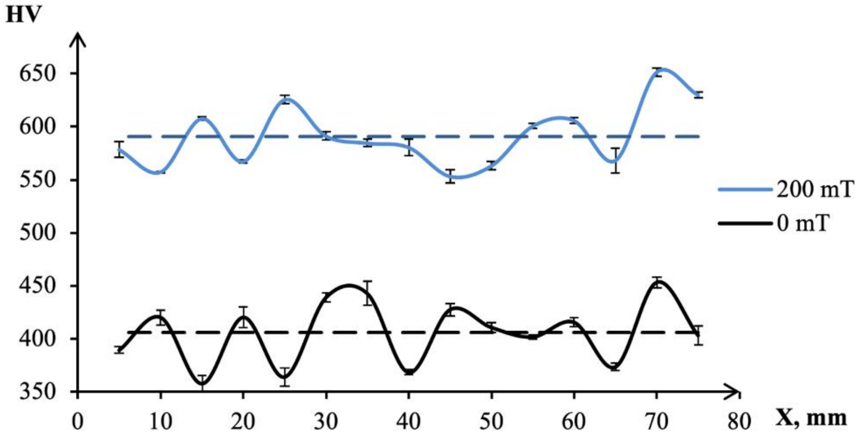

Figure 6 - The microhardness of wire arc additive manufactured steel 9CrMoV-N affected by a magnetic field and unexposed to it vs. a distance to the base. Dashed lines indicate the mean values of the microhardness.

3.4 Corrosion testing results

Figure 7 visualizes samples after the corrosion testing. The surface of tested samples appears to be dull without any visible corrosion products. The principal criteria accepted in the corrosion testing include a weight loss of samples and a corrosion rate. There was no a weight loss in a sample produced without a magnetic field. A weight loss in a sample exposed to a magnetic field when fabricated was determined to be 0.0007 g; its annual rate of corrosion is 0.08 mm per year. Thus, we suggest both samples have passed the corrosion testing.

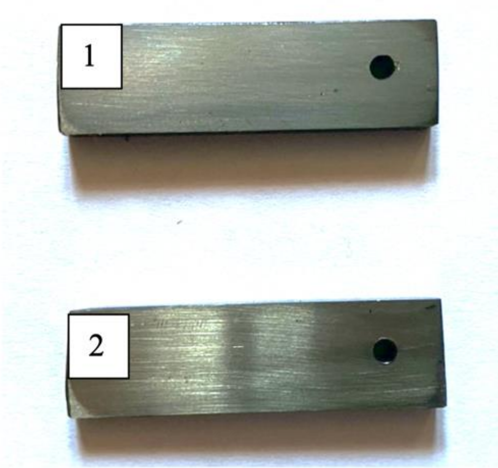

Figure 7 - Samples of steel 9CrMoV-N before and after corrosion resistance testing (1 – produced without a magnetic field, 2 – in a magnetic field)

Conclusion

In this study, we obtained ferrite-martensite steel 9CrMoV-N samples via wire arc additive manufacturing. The effect of a constant magnetic field with a value of induction 0.2 T on the microstructure, microhardness, and corrosion properties of samples was explored. The microstructure of samples under study fabricated in and out of a magnetic field appears to be a lath martensite microstructure. Defects in the form of spherical pores were detected in the microstructure of both types of samples. However, the magnetic field application reduced the number of pores by 6.12% and their size by 41.81%. Under the action of a magnetic field in the wire arc additive manufacturing of steel

9CrMoV-N we observed the 1.5 times refinement of grains against samples formed without a magnetic field. Another result of applying a magnetic field in wire arc additive manufacturing is 1.5 times increase in the mean microhardness by contrast to samples not affected by a magnetic field. An X-ray diffraction analysis revealed main phases $Mn_{23}C_6$, Mn_7C_3, NbN, VN, VC, Fe_7W_6, Fe_7C_3, Fe_3C, Cr_7C_3, Cr_2N and $Cr_{23}C_6$ both in samples exposed and unexposed to a magnetic field. The corrosion testing outcomes demonstrated that a sample fabricated without a magnetic field not experiencing weight loss, however weight loss to be 0.0007 g in a sample affected by a magnetic field. As a result of corrosion tests, the samples' surface was dull, although no corrosion signs were detected.

To summarize, the application of a constant magnetic field brings about the refinement of grains, reduces the number of pores and their size, increases the microhardness, makes no difference for the phase composition and corrosion characteristics of wire arc additive manufactured steel 9CrMoV-N.

Acknowledgments

Funding: This work was supported by the National Natural Science Foundation of China, grant no. 51975419. We greatly appreciate the assistance provided by OOO Research and development manufacturing company “Valma” (Samara) in the carrying out corrosion tests.

References

1. P.J. Ennis, A. Czyrska-Filemonowicz, Recent advances in creep-resistant steels for power plant applications, Sadhana - Acad. Proc. Eng. Sci. 28 (2003) 709–730. https://doi.org/10.1007/BF02706455.

2. R.G. Faulkner, J.A. Williams, E. Gonzalez Sanchez, A.W. Marshall, Influence of Co, Cu and W on microstructure of 9%Cr steel weld metals, Mater. Sci. Technol. 19 (2003) 347–354. https://doi.org/10.1179/026708303225009652.

3. S.I. Porollo, A.M. Dvoriashin, Y. V. Konobeev, F.A. Garner, Microstructure and mechanical properties of ferritic/martensitic steel EP-823 after neutron irradiation to high doses in BOR-60, J. Nucl. Mater. 329–333 (2004) 314–318. https://doi.org/10.1016/j.jnucmat.2004.04.310.

4. Y.-C. Huang, C.-S. Tsao, S.-K. Wu, C. Lin, C.-H. Chen, Nano-precipitates in severely deformed and low-temperature aged CoCrFeMnNi high-entropy alloy studied by synchrotron small-angle X-ray scattering, Intermetallics. 105 (2019) 146–152. https://doi.org/https://doi.org/10.1016/j.intermet.2018.12.003.

5. C. Guo, S. Liu, R. Hu, C. Liu, F. Chen, Heat-Resistant Steel Produced by Wire Arc Additive Manufacturing, 2020 (2020).

6. R. Chen, P. Jiang, X. Shao, G. Mi, C. Wang, Effect of magnetic field on crystallographic orientation for stainless steel 316L laser-MIG hybrid welds and its strengthening mechanism on fatigue resistance, Int. J. Fatigue. 112 (2018) 308–317. https://doi.org/10.1016/j.ijfatigue.2018.03.034.

7. S. Konovalov, D. Zagulyaev, X.-Z. Chen, V. Gromov, Y. Ivanov, Variations in defect substructure and fracture surface of commercially pure aluminum under creep in weak magnetic field, Chinese Phys. B. 26 (2017). https://doi.org/10.1088/1674-1056/26/12/126203.

8. B. Wu, Z. Pan, D. Ding, D. Cuiuri, H. Li, J. Xu, J. Norrish, A review of the wire arc additive manufacturing of metals: properties, defects and quality improvement, J. Manuf. Process. 35 (2018) 127–139. https://doi.org/10.1016/j.jmapro.2018.08.001.

9. C. Gao, X. Chen, C. Su, X. Chen, Location dependence of microstructure and mechanical properties on wire arc additively manufactured nuclear grade steel, Vacuum. 168 (2019) 108818. https://doi.org/10.1016/j.vacuum.2019.108818.

10. Y. Hu, L. Wang, J. Yao, H. Xia, J. Li, R. Liu, Effects of electromagnetic compound field on the escape behavior of pores in molten pool during laser cladding, Surf. Coatings Technol. 383 (2020) 125198. https://doi.org/10.1016/j.surfcoat.2019.125198.